High-T_c superconductivity in entirely end-bonded multi-walled carbon nanotubes

J.Haruyama[1,4,], N.Kobayashi[1], I.Takesue[1,4], S.Chiasi[2], S.Maruyama[2], T.Sugai[3,4], H.Shinohara[3,4]*

[1]Aoyama Gakuin University, 5-10-1 Fuchinobe, Sagamihara, Kanagawa 229-8558 Japan
[2]Tokyo University, 7-3-1 Hongo, Bunkyo-ku, Tokyo 113-0033 Japan
[3]Nagoya University, Furo-cho, Chigusa, Nagoya 464-8602 Japan
[4]JST-CREST, 4-1-8 Hon-machi, Kawaguchi, Saitama 332-0012 Japan

***** Corresponding author; J-haru@ee.aoyama.ac.jp

Abstract

We report that entirely end-bonded multi-walled carbon nanotubes (MWNTs) within Tomonaga -Luttinger liquid (TLL) states at high temperatures can show superconductivity with the transition temperature T_c as high as 12K that is approximately 50-times larger than those in ropes of single-walled nanotubes. We find that emergence of this superconductivity is very sensitive to junction structures of Au electrode/MWNTs. This indicates that MWNTs with optimal numbers of electrically activated shells can allow the superconductivity that overcomes the TLL sates, due to intershell effects. This superconductive MWNT will lead to molecular quantum computation and teleportation systems.

1. INTRODUCTION

One-dimensional (1D) systems face some obstructions that prevent the emergence of superconductivity, such as a Tomonaga-Luttinger liquid (TLL) [1][2], spin fluctuation, small density of state due to van-Hove singularity (VHS), and Peierls transition (charge-density waves). A carbon nanotube (CN), an ideal 1D molecular conductor, is one of the best candidates for investigating this possibility. Although a variety of intriguing quantum phenomena has been reported in CNs, only two groups have reported intrinsic superconductivity (e.g., with a transition temperature (T_c) as low as T_c = ~0.2K [3] and that identified only from the Meissner effect [4]) only in single-walled CNs (SWNTs) (ropes) to the best of our knowledge. In addition, those correlations with 1D phenomena, particularly with TLL state, which may destroy Cooper pairs, have never been clarified.

TLL states, which are a non Fermi-liquid state arising from an 1D repulsive electron-electron interaction and exhibit some exotic behaviors (e.g., spin-charge separation), have been frequently reported by observing power laws in the relationships of conductance vs. energies in both multi-walled carbon nanotubes (MWNTs) [1][5] and single-walled carbon nanotubes (SWNTs) [2], with various power α. The observed correlation exponent g, which denotes the strength of an electron-electron interaction (e.g., $g < 1$ and $g > 1$ signify the repulsive and attractive Coulomb interactions, respectively) and determines α, as low as ~ 0.2 stressed the presence of a strong repulsive Coulomb interaction in carbon nanotubes (CNs).

Does this strong repulsive Coulomb interaction prevent the emergence of Cooper pairs and superconductivity? Refs. [6]-[9] predicted that the correlation of a TLL state with superconductivity is highly sensitive to phonon modes, the coupling of them with electrons, and structures of ropes of CNs, allowing for the appearance of superconductivity. However, this has not yet been experimentally verified. To the best of our knowledge, confirmed reports of superconductivity in 1D conductors are only in organic materials [10].

In refs. [11] – [13], we have successfully realized end-bonding of MWNTs synthesized in nanopores of alumina templates. Recently, we also realized proximity-induced superconductivity (PIS) by end-bonding MWNTs, which were prepared using the same method, by Nb electrode [11][12]. They proved that the Cooper pairs could be effectively transported without destruction only through the highly transparent interface of the CNs/Nb junctions obtained by this end-bonding. Such an entire end-bonding has never been carried out in conventional FET structures using CNs.

2. EXPERIMENTAL RESULTS AND DISCUSSIONS

Following the method with alumina templates but employing some specified conditions [14] (Fe/Co catalyst and Methanol gas), we synthesized arrays of Au/MWNTs/Al junctions (Fig.1(a)). Figure 1(d) shows a plane transmission electron microscope (TEM) image of the array shown in (a). MWNTs are clearly visible in many pores. In the inset, a high-resolution cross-sectional TEM image of a MWNT is shown. Structures of this MWNT is similar to those in conventional MWNTs. It also includes no Fe/Co catalyst, which tends to destroy Cooper pairs, in the entire region. Figure 1(e) shows a result of resonance Raman measurements of the MWNTs. Only a large peak is observed significantly around 1600 cm^{-1} (the so-called G-band). This strongly indicates that the MWNTs have high quality without defects. Absence of ferromagnetic catalyst and defects in the MWNTs with high quality are very different from those in our previous studies [11]-[13].

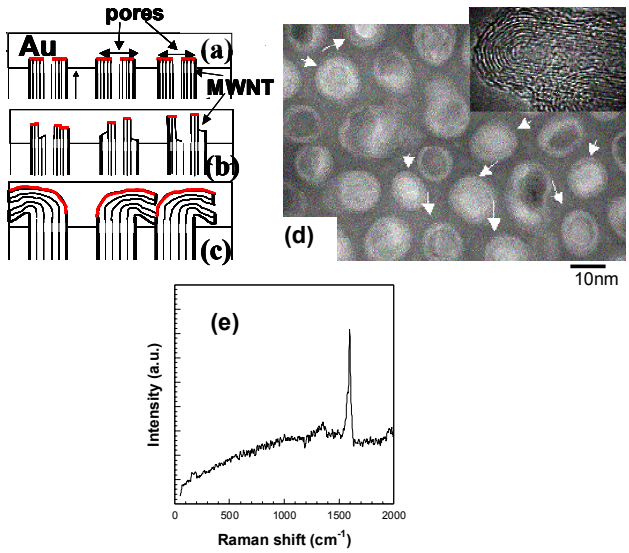

Figure 1: Schematic cross-sections of Au/MWNTs interfaces in Au/MWNTs/Al junctions prepared in alumina templates with **(a) entire Au-end (b) partial Au-end** and **(c) Au-bulk** junctions. Red lines are the interfaces where can have electrical contacts to Au electrodes. The lengths of MWNTs are ~ 0.6 μm. Quasi-four terminal measurements were performed by attaching lead lines to Au electrode and Al substrate. Approximately 1000 MWNTs exist under an electrode. **(d)** Plane TEM image of the MWNT array, which were shown in Fig.1(a) and used for Fig.2(a). This image was observed around the tope end of an alumina template. MWNTs were shown by arrows. **Inset:** High-resolution cross-sectional TEM image of a MWNT, which were observed by resolving the alumina template and purifying the solution. The MWNT has a diameter of ~7.4 nm, the number of shells of 9, the shell thickness of ~2.7 nm, and the intershell spacing of ~3.4 Å. **(e):** A result of resonance Raman measurements of the MWNT by laser energy of 2.41 eV.

We prepared three-different types of Au electrode/MWNTs junctions using this MWNT [15] in order to investigate importance of end-bonding and reveal influence of intershell effects on superconductivity and TLLs; i.e., **(1)** Entire Au-end junctions (Fig.1(a)), **(2)** Partial Au-end junctions (Fig.1(b)), and **(3)** Au-bulk junctions (Fig.1(c)). For (1), it was already proven that this method could allow making contact of Au electrode to all the shells of MWNTs in refs. [11]-[13] (red lines in Fig.1(a)), resulting in the entire end-bonding. In contrast, for (2), only partial shells could have contacts to Au (Fig.1(b)). For (3), only the outermost shell could have contact to the Au electrode in this junction as reported in previous studies [5][19] (Fig.1(c)). Each structure was confirmed by high-resolution cross-sectional TEM observations.

Figure 2 shows the zero-bias resistance (R_0) as a function of temperatures for the three different junctions as mentioned above. One can confirm an apparent superconducting transition with the onset T_c as high as 12K and the temperature ($T_c(R = 0)$), at where the R_0 drops to 0 Ω, as high as T = 7.8K only in the entire Au-end junction sample (main panel of Fig.2(a)). These values for onset T_c and $T_c(R = 0)$ are at least approximately 25- and 40-times, respectively, higher than those reported in SWNT ropes [3]. Six samples have exhibited such high-T_c features (i.e., onset T_c = 6 ~ 12K) to date. On the contrary, in the partially end-bonded sample, only a small R_0 drop (i.e., a sign of superconductivity) was observable below T= ~3.5K without a R_0 decrease down to 0 Ω at T = 1.5K (main

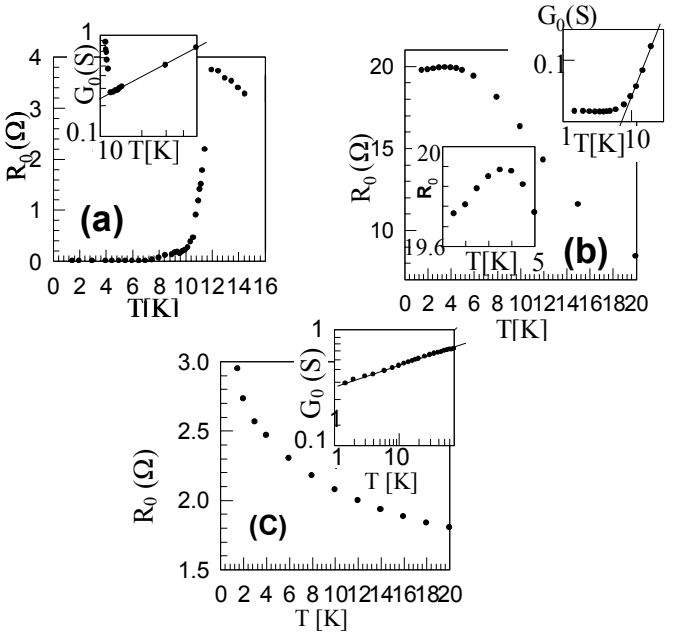

Figure 2: Zero-bias resistance (R_0) as a function of temperatures for three different junctions; **(a)** for the entire Au-end junction, **(b)** for the partial Au-end junction, and **(c)** for the Au-bulk junction. The residual resistance of ~ 1 ohm has been subtracted in the figures.**Insets of each figure** (except for lower inset of (b)): doubly logarithmic scales of zero-bias conductance (G_0) as a function of temperatures for each main panel. The solid lines are provided just to the eyes. **Lower inset of (b):** Expansion of the main panel at T ≤ 5K in normal scales.

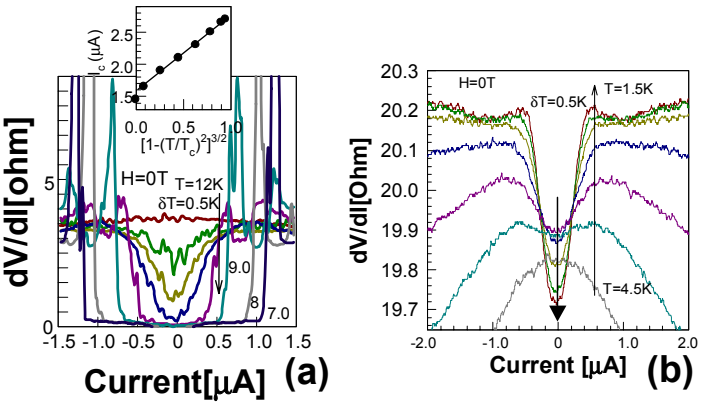

Figure 3: Differential resistance as a function of current at zero magnetic fields for different temperatures (**(a)** for the entire Au-end junction, **(b)** for the partial Au-end junction). The numbers noted on each curve denote the temperatures in Kelvin. In (a), oscillations of resistance peaks similar to those in refs. [3][11] (interpreted as a phase slip) are observable in the large current regions at T ≤ 8.5 K. **Inset of (a):** Relationship of critical current (I_c) vs temperature normalized for comparison with the Ginzburg-Landau critical current behavior. The solid line is provided just to the eyes.

panel and lower inset of Fig.2(b)). Most of samples have shown this-type sign of superconductivity to date. No R_0 drop was observable in measured entire temperatures in the Au-bulk junction sample (Fig. 2(c)).

Figure 3 shows the differential resistance as a function of current for different temperatures. A low and broad resistance peak due to TLL state (discussed later in this letter) exists at T = 12K in the entire Au-end junction sample (Fig.3 (a)). This peak disappears suddenly and a resistance drop appears T = 11.5K. The depth and width of this resistance drop monotonically increase as the temperature decreases, corresponding to Fig.2(a). The value of superconducting gap $\Delta \approx 1.15$ meV observed at T = 8K in this sample is in excellent agreement with the Bardeen-Cooper-Schrieffer (BCS) relation $\Delta = 1.76kT_c$, when $T_c(R=0) = 7.8$K is used. Moreover, the behaviors of critical current (I_c) in normalized temperatures as shown in the inset of (a) is also in excellent agreement with the Ginzburg-Landau (GL) critical current behavior for a homogeneous order parameter, $I_c \propto [1- (T/T_c)^2]^{3/2}$ [17]. These suggest that the observed superconductivity is strongly associated with the BCS type.

In contrast, the behavior in the partially end-bonded sample (Fig.3(b)) differs greatly from that observed in Fig.3(a), since it includes the temperature dependence of the resistance peak as follows. A large and broad resistance peak due to the TLL is observable at T = 4.5K. It broadens as the temperature decreases and mostly disappears at T = 2.5K. In contrast, a resistance drop with a narrow width begins to be observed at the center of the peak at T = 4 K and the depth monotonically increases in a temperature decrease. A corresponding drop in the total R_0 can be observed only below T = 3.5 K (Fig. 2(b)), reflecting the superposition of these resistance peak and drop. The residual resistance is still large even at T = 1.5 K due to this resistance peak. Importantly, presence of this resistance peak prevents both the emergence of superconducting gap at T ≥ 4.5 K and the R_0 drop at T ≥

3.5K.

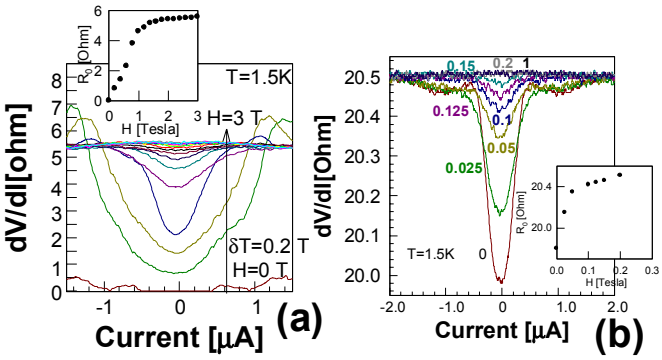

Figure 4: Differential resistance as a function of current at T = 1.5K for different magnetic field (**(a)** for the entire Au-end junction, **(b)** for the partial Au-end junction). The number noted on each curve is the magnetic field in Tesla, which was applied perpendicular to the tube axis. **Insets:** R_0 vs .magnetic field relationships

Figure 4 shows the differential resistance as a function of current for different magnetic fields (H). The drastic increase of R_0 from zero fields with a field increase observed in the entire Au-end junction sample (inset of Fig.4(a)) differs greatly from that in SWNT ropes [4]. Figure 4(b) in the partially end-bonded sample also exhibits a qualitatively similar increase in R_0. This low critical field implies that the observed superconductivity is either type-I or type-II without defects for pinning of the magnetic fluxes penetrating the MWNTs. Alternatively, this may indicate the presence of strong electron-acoustic phonon coupling, as reported by Ando et al. [18], since a huge magnetoresistance was predicted to have appeared even under small magnetic fields in CNs with strong electron-acoustic phonon coupling. Such coupling can cause superconductivity with high T_c

One of the origins for the superconductivity observed here is the effective transport of Cooper pairs through the highly transparent interface of the Au-end junctions as proven in refs. [11]-[13]. However, the observation of the power law behaviors for the different junction types (insets of Fig.2) reveals presence of an essential mechanism for this, which is strongly associated with competition between superconductive phase and TLL states as mentioned in introduction.

The exponent α of the power laws in TLLs is extremely sensitive to the junction conditions between electrodes and CNs. Ref. [1] reported a power α for tunneling from an Au electrode to the bulk (α_{bulk} = ~ 0.3) and to the end (α_{end} = ~ 0.7) of the MWNTs within the large channel-number TLL state as well as $\alpha_{end\text{-}bulk}$ and $\alpha_{end\text{-}end}$ between two CNs [22]. The exponent α = ~ 0.7, ~ 0.8, and ~ 0.3 estimated from the power laws shown in the insets of Fig.2 (a), (b) and (c), respectively, are in good agreement with α_{end} and α_{bulk}. This result proves the actual presence of Au-end and Au-bulk junctions in the systems, as shown in Fig.1(a)-(c), as well as the presence of TLLs in these MWNTs. In addition, the resistance of the sample for Fig.1(b) was approximately ten-times larger than that for Fig.1(a) as shown in Fig.2(a) and (b) as well as those at a room temperature. This means a poor Au/MNTs junction in Fig.1(b)-sample and supports the presence of Fig.1 junctions.

Only the TLL was observed without superconductivity in all the temperatures (Fig.2(c)) in the Au-bulk junction sample, in which the outermost shell made contact to the Au electrode (Fig.1(c)). This is consistent with refs. [5] and [20], which reported that only the (second) outermost shell became electrical active in the Au-bulk junction of CN-FET structures and that exhibited TLLs in MWNTs. This is why most of MWNT-FETs in previous reports have not exhibited superconductivity. This result means that single shell within the TLL state cannot take a transition to superconductive phase unlike previous predictions [6].

In contrast, it should be noted that the TLL abruptly disappeared and the superconductive phase simultaneously emerged at high T_c=12K with a temperature decrease in the entire Au-end junction sample (Fig.2(a)), whereas the transition from the TLL state to the superconductive phase was gradual resulting in the low T_c in the partial Au-end junction sample (Fig.2(b)). Here, the entire end-bonding of MWNTs could make contact to all the shells (Fig.1(a)) and, thus, made the entire shells to be electrically active. In the partial Au-end junctions, only partial number of shells that could be end-bonded to Au (Fig.1(b)), were electrically active. These indicate that the significant differences in correlations of the TLL with the present superconductivity at least have strong correlation

with the number of electrical active shells (N) of the MWNTs (i.e., N=1 for Fig.2(c), N=9 for Fig.2(a), and 1 < N < 9 for Fig.2(b)). This also strongly indicates that intershell effects of the MWNTs play the key role for the emergence of high-T_c superconductivity with competing to the TLLs.

In fact, the intershell effects in MWNTs have been discussed for the TLLs in refs. [1][19]. Egger [19] predicted the TLL in low-energy theory of MWNTs, taking into account the (externally unscreened) long-ranged Coulomb interaction, internal screening effects, and intershell electron tunneling (hopping). This TLL was sensitive to the values of N of the MWNT, resulting in Fermi liquid behaviors as the value of N increased. The value of N = 9 in the present MWNT is within the upper limit for this TLL theory. In contrast, no previous study predicted a superconducting transition in MWNTs within the TLL states. However, because the theory [19] was applicable also to SWNT ropes, one can discuss correlation of superconductivity with the TLLs, replacing the N of MWNTs (i.e., intershell effects) to the number of SWNTs included in SWNT ropes (i.e., intertube effects).

The importance of the intertube effects for the appearance of superconductivity associated with TLLs has been theoretically pointed out in ropes of SWNTs [7]. Based on ref.[7] and replacing intertube effect to intershell effect, the competition between the TLLs and the superconducting phase shown in Figs.2 and 3 can be qualitatively explained as follows. The TLLs are weakened by intershell charge coupling (i.e., coupled TLLs; sliding TLLs [16]) due to prohibition of the intershell electron hopping because of presence of misalignment of carbon atoms between shells owing to different chiralities and diameters. In contrast, an intrashell short-range attractive Coulomb interaction is enhanced by allowing the intertshell Cooper-pair hopping in a temperature decrease [7][8]. These differences become apparent as the values of N increase.

Based on this model, in Fig.2(c), TLL easily overcomes the short-range attractive Coulomb interaction because of N = 1, resulting in the TLL state without a superconducting transition. In contrast, in Figs.2(a) and 3(a), the intrashell attractive Coulomb interaction rapidly grows with decreasing temperatures because of N = 9, while the TLLs are drastically reduced. These effects result in the abrupt change from the resistance peak due to the TLLs at T = 12 K to the superconducting gap at T=11.5 K (Fig.3(a)), and this change corresponds to the abrupt appearance of superconducting transition (R_0 drop) from T_c = 12 K to T = 10 K (Fig.2(a)). The situations for N = 1 and N = 9 are competed in Figs.2(b) and 3(b), because 1 < N < 9. The resistance peak due to the TLLs and the resistance drop due to the superconducting phase are competed as mentioned for Fig.3(b) and the corresponding gradual change in R_0 is observable in Fig.2(b). The temperature region between 10 K and 3.5 K in Fig.2(b) can be considered as a competition region between the TLL states and the superconductive phase in this term.

For a quantitative interpretation, difference in strength of the intertube and intershell effects is important. The higher T_c in N = 9 reported here indicates that the latter is much stronger. Besides, clarification of the correlation between N, T_c, and α is also crucial in this viewpoint. The importance of interlayer effects has also been pointed out in 2D-layered superconductors, e.g., MgB_2, high-T_c oxide superconductors, and graphite-related superconductors (graphite-intercalated compounds and fullerenes). Influence of curvature (i.e., tube structure) in MWNTs on π - σ orbital coupling and electron-phonon interaction, and those influences on T_c are expected to be revealed compared with these superconductors. Furthermore, VHSs in each single shell are superposed in a MWNT, resulting in a peak–width broadening in VHS. Correlation of this effect with T_c should be clarified, because this may increase density of states around Fermi levels. It is also indispensable to improve how to reproducibly make the entire end-bonding in order to obtain higher reproducibility of high-T_c samples.

Finally, we discuss application of this superconductive MWNT to molecular quantum computation. Ref. [21] indicated that the TLLs of CNs tended to separate Cooper pairs, which are injected from superconductor electrode, into individual spins in a hybrid system of one superconductor and two CNs and the separated spins could be injected into different CNs. If Cooper pairs in CNs actually have a strong entanglement [12][20],

separated spins retain a strongly entangled state crossing the different CNs. This results in realization of molecular spin-entanglers. Moreover, Loss et al. also predicted that efficiency of Cooper pair splitting became higher as dimension of superconductor electrode decreased [21]. Because dimension of the MWNT is one, much higher efficiency can be obtained when our superconductive MWNT is used instead of a superconductor electrode.

3.Acknowledgments

We greatly thank J.Akimitsu, R.Saito, S.Saito, S.Tarucha, Y.Iye, M.Tsukada, J.Gonzalez, H.Bouchiat, E.Demler, R.Barnett, R.Egger, G.Loupias, J.-P. Leburton, D.Loss, and M.Dresselhaus for fruitful discussions and encouragement. We also thank N.Sugiyama for the nice plane TEM image and J.Mizubayashi for the help in Raman spectrum measurements..

References

1. A.Bachtold, C.Shonenberger, et al., Phys.Rev.Lett. 87, 166801 (2001)
2. M.Bockrath, et al., Nature 397, 598 (1999); H.Ishii, H.Kataura, et al., Nature 426, 540 (2003)
3. M. Kociak, H. Bouchiat, et al., Phys. Rev. Lett. 86, 2416 (2001)
4. Z. K. Tang, et al., Science 292, 2462 (2001)
5. A.Bachtold, et al., Nature 397, 673 (1999); M.R.Buitelaar, et al., Phys.Rev. Lett. 88, 156801 (2002)
6. D.Loss and T.Martin, Phys. Rev. B 50, 12160 (1994-II)
7. J.Gonzalez, Phys.Rev.Lett. 88, 076403 (2002); A.Sedeki, et al., Phys.Rev.B 65, 140515(R) (2002); J.Gonzalez, Phys.Rev.Lett. 87, 136401 (2001)
8. De Martino and R.Egger, Phys.Rev.B 67, 235418 (2003)
9. J.Gonzalez, et al., Phys.Rev. B 63, 134421 (2001)
10. I.J.Lee, et al., Phys. Rev. Lett. 78, 3555 (1997)
11. J.Haruyama, et al., Phys.Rev.B 68, 165420 (2003); Appl.Phys.Lett. 84, 4714 (2004); Microelectronics Journal 34, 537 (2003); Physica C 408, 85 (2004)
12. J.Haruyama, et al., Phys.Rev.Lett. In submission; Physica Stat. Sol. (b) 242(2), 265 (2005)
13. J. Haruyama, et al., Phys. Rev. B 65, 33402 (2002); Pys.Rev.B, 073406 (2001)
14. S. Maruyama, et al., Chem. Phys. Lett. 360, 229 (2002).
15. Electrochemical deposition time of Fe/Co catalyst into the bottom of the pores and time of ultrasonic cleaning for cutting the MWNTs [11], which grew above the pores and accumulated on the template surface, were optimized for each structure.
16. A.Vishwanath and D.Carpentier, Phys.Rev.Lett. 86, 676 (2001)
17. M.Tinkam, *Introduction to Superconductivity* (McGraw-Hill, New York 1996)
18. H.Suzuura and T.Ando, Phys.Rev.B 65, 235412 (2002)
19. R.Egger, Phys.Rev.Lett. 83, 5547 (1999)
20. M.R.Buitelaar, C.Shonenberger, Phys.Rev. Lett. 89, 256801 (2002)
21. I.Takesue, T.Akazaki. J.Haruyama., H.Takayanagi, et al., Physica E 24, 32 (2004); P.Recher and D. Loss, Phys. Rev. B 65, 165327 (2002); C.Bena et al., Phys.Rev.Lett.89, 037901 (2002)
22. This interpretation for the origin of power laws is still on debating stage. A Coulomb blockade strongly coupled with its external electromagnetic environment and a phenomenon related to 1D localization may explain them.